



Contents lists available at ScienceDirect

Journal of Photochemistry and Photobiology A: Chemistry

journal homepage: www.elsevier.com/locate/jphotochem

Photochemical dissociation of HOBr. A nonadiabatic dynamics study

Saadullah G. Aziz^a, Abdulrahman O. Alyoubi^a, Shaaban A. Elroby^{a,b}, Rifaat H. Hilal^{a,c,*}^a Chemistry Department, Faculty of Science, King Abdulaziz University, Jeddah B.O. 208203, Saudi Arabia^b Chemistry Department, Faculty of Science, Beni-Suef University, Beni-Suef 6251, Egypt^c Chemistry Department, Faculty of Science, Cairo University, Cairo 12613, Egypt

ARTICLE INFO

Article history:

Received 31 January 2016

Received in revised form 24 February 2016

Accepted 27 February 2016

Available online 16 March 2016

Keywords:

HOBr

Excited state dynamics

TDDFT

Photodissociation

Non-adiabatic dynamics

ABSTRACT

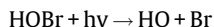
A number of single-reference post Hartree-Fock methods, namely CIS, symmetry adopted cluster configuration interaction (SA-CI), equation of motion coupled cluster (EOM-CCSD) and time-dependent density functional theory (TDDFT), were used to investigate the excited state properties and photochemical dissociation of hypobromous acid, HOBr. Results are in good agreement with experimental data. The decay of the excited states of HOBr in the gas phase was examined by simulating the UV photoabsorption spectrum and nonadiabatic dynamics at the TDDFT M06-2X level of theory. The spectrum, composed of 10 excited states, was simulated with the nuclear ensemble approximation, sampling a Wigner distribution with 500 points. Dynamics simulations were done with the surface hopping method, started in two separate spectral windows, at 4.0 ± 0.25 eV and 8.0 ± 0.25 eV, to be compared to experimental UV spectral data. Three hundred trajectories were considered from each of these windows according to their excitation probabilities. The excited-state lifetime was determined. The main photochemical channel observed were HO and Br eliminations, representing 67% of all processes.

© 2016 Elsevier B.V. All rights reserved.

1. Introduction

The important role played by the different bromine species in ozone depletion, was recently recognized [1,2]. This is especially important in the Arctic spring and in areas where there exist high concentration of HOX species (e.g. OH radical) [3–6]. The depletion of ozone by BrO and OH radical was investigated in the laboratory [7–9] where it was concluded that such a process would increase the recycling of bromine.

The photolysis of HOBr was suggested to be the most important channel in this respect [10], and may be written as



This photodissociation reaction was investigated near the threshold of dissociation at 490 and 510 nm. Characterization of the OH photofragment was carried out via Doppler and polarization spectroscopy using laser-induced fluorescence [11].

The UV-vis spectrum of HOBr was, measured over the 200–420 nm range. Two main absorption bands centered near 280 and

350 nm were observed [12–14]. A third long wave length band, centered near 440 nm was later detected by monitoring the yield of OH radicals as the wavelength of an excitation laser is scanned over the region from 440 to 650 nm. This band has been assigned to a transition to a triplet state, and although its peak absorption cross section is very small, its influence on determining the photochemical lifetime of HOBr is large due to its proximity to the peak of the solar actinic flux [9].

Motivated by the fact that very little is known about the photolysis of HOBr, its photochemical and photophysical dissociation mechanism, the present research project is launched with a focus on the calculation of excited state properties, using different correlated single-reference methods. The reduced computational cost of such methods has allowed us to extend our investigations to nonadiabatic dynamics processes [1] starting at highly excited states (S_7 – S_{11}), where photochemical reactions of HOBr has been experimentally studied. It should be noted here that, although the molecule at hand is triatomic small and can in principle be handled by quantum dynamics, yet inclusion of this number of excited states in the quantum dynamics simulations is practically impossible. Based on these nonadiabatic dynamics simulations, we have been able to provide a much better insight into the photolysis of this molecule.

* Corresponding author at: Chemistry Department, Faculty of Science, King Abdulaziz University, Jeddah B.O. 208203, Saudi Arabia.

E-mail addresses: saziz@kau.edu.sa (S.G. Aziz), aalyoubi@kau.edu.sa (A.O. Alyoubi), skamel@kau.edu.sa (S.A. Elroby), rhilal@kau.edu.sa (R.H. Hilal).

2. Computational details

The ground-state geometry was optimized at the MP2 level with the aug-cc-pVTZ basis set [17,18] using GAUSSIAN 09 [19]. This geometry was used for further calculations of the vertical excitations using the same basis set. The diffuse character of this basis set enables it to give the correct description of Rydberg orbitals. Excited state calculations started at the low level CIS [20], and then the more accurate and involving symmetry adopted cluster configuration interaction (SA C-Cl) [16] and equation of motion coupled cluster with single and double excitations (EOM-CCSD) [21], methods. TDDFT (time-dependent density functional theory) calculations were also carried out with M06-2X [22] and ω B97XD [23] functionals, using GAUSSIAN 09. For each method, 10 singlet excited states were computed. The Cs symmetry was enforced in all static calculations.

In a second part of the investigation, relaxed potential energy-curve calculations along two internal coordinates, namely the Br O-H and the HO-Br coordinates, have been performed. The ground and 10 excited states ($5A'$ and $5A''$) have been computed on ground-state relaxed geometries. The calculations have been carried out at the EOM-CCSD method.

In the last part of the study, UV photoabsorption spectrum and nonadiabatic dynamics simulations were carried out to understand the ultrafast decay of the excited states of HOBr in the gas phase. Computations were performed using Newton-X program package [24,25] at the TDDFT/M06-2X level of theory. In order to simulate the photoabsorption spectrum, 500 points were sampled with the nuclear ensemble approximation [25]. The same number of excited states computed in the relaxed potential energy curves (10) was considered here. Dynamics simulations were started in two spectral windows at 4.0 ± 0.25 and 8.0 ± 0.25 eV. Three hundred trajectories were stochastically sampled from each of these windows according to their excitation probabilities. Dynamics simulations were done with the surface hopping method [26,27]. Classical equations were integrated with 0.5 fs time-step, while quantum equations were integrated with 0.025 fs. For the quantum integration, all necessary quantities were interpolated between classical steps. Nonadiabatic effects between excited states were taken into account by the fewest switches algorithm [28] with decoherence corrections ($\alpha = 0.1$ Hartree) [29]. Nonadiabatic couplings between excited states were computed by finite differences with the method proposed by Hammes-Schiffer and Tully [30].

3. Results and discussion

3.1. Excitation energies and oscillator strengths

The results obtained for vertical-excitation energies, oscillator strengths, and state assignments computed with the TD-M06-2X and ω B97XD functionals and EOM-CCSD method, are shown in Table 1. With respect to the vertical excitation energies, all three methods are in good agreement with the observed spectrum of HOBr. All calculated excited states are in the range up to >10 eV. Two main band systems dominate the computed spectrum. The first long wave length band system is centered on 3.5 eV and is composed of one configuration, namely the HOMO-LUMO transition. The MO's involved are displayed in Fig. S3 of the supplementary material (SM). These KS MO's were computed at the M06-2X/aug-cc-pVTZ level of theory. For visualization and to make the assignment of the delocalized KS MO's more straightforward, a full natural orbital treatment (nbo) has been performed and the resulting orbitals are those displayed in Fig. S3. The long wave length absorption at 3.39 eV is of very low intensity as compared to the short wave length one. This transition is of the combination of $n_{Br} - Ryd$ and $\sigma - \sigma^*$ type localized on the O-Br bond region. Whereas, the short wavelength absorption, which spans the 7.5–8.5 eV range, may be attributed to a transition from a $n_{Br\pi} - \sigma^*$.

The Symmetry Adapted Cluster/Configuration Interaction (SA C-Cl) methods of Nakatsuji and coworkers [21] have been also used to explore the excited state space for the singlet, triplet and ionized states of HOBr. Results are summarized in Table 2. SA C-Cl computations predicted two singlet states, one triplet and two ionized states in the region <11.5 eV. The singlet states are heavily mixed with several configurations. These singlet states are contaminated by 1.7% and 0.53% of doublet states. The triplet state, on the other hand, is pure. The first ionized state is of symmetry A' and is characterized by ionization potential (I.

Table 2
Transition energies of singlet, triplet and ionized states of HOBr computed at the SA C-Cl/aug-cc-pVTZ level of theory.

Spin	symm	E,eV	Transition dipole, au			f
			x	y	z	
S_2	A'	4.635	-0.0852	0.1695	0.0000	0.0041
S_1	A''	3.776	0.0	0.0	0.0085	0.000
T_1	A'	3.790	0.0	0.0	0.0	0.0
Ionized cation doublet	A'	11.324				0.955
	A''	10.604				0.948

Table 1
Vertical-Excitation Energies, Oscillator Strengths and main configurations obtained for HOBr with different methods and aug-cc-pVTZ basis Set.

ω B97-XD					M06-2X					EOM-CCSD				
$\Delta E, eV$	Sym	F	Assignment	weight	$\Delta E, eV$	Sym	f	Assignment	weight	$\Delta E, eV$	Sym	f	Assignment	weight
3.58	A''	0.002	$n_{Br\pi} - \sigma^*$	0.70	3.45	A''	0.001	$n_{Br\pi} - \sigma^*$	0.68	3.77	A''	0.002	$n_{Br\pi} - \sigma^*$ $n_{\pi} - \sigma^*$	0.32
4.43	A'	0.018	$n_{Br} - \sigma^*$	0.70	4.33	A'	0.017	$n_{Br\pi} - \sigma^*$	0.68	4.63	A'	0.02	$n_{Br} - \sigma^*$	0.45
6.77	A''	0.006	$n_{Br\pi} - \sigma^*$	0.60	6.69	A''	0.012	$n_{Br\pi} - \sigma^*$	0.64	7.015	A''	0.02	$n_{Br} - \sigma^*$	0.33
6.88	A''	0.011	$n_O - \sigma^*$	0.25	7.40	A'	0.037	$n_{Br} - \sigma^*$	0.66	7.78	A'	0.05	$n_{Br} - \sigma^*$	0.47
8.43	A'	0.12	$n_{Br\pi} - \sigma^*$	-0.22	8.60	A'	0.081	$\sigma - \sigma^*$	-0.38	8.42	A''	0.08	$\sigma - \sigma^*$	-0.39
9.11	A''	0.002	$n_{Br\pi} - 5p$	0.60	9.15	A''	0.029	$n_{Br} - Ryd$	0.48	8.64	A'	0.18	$n_{Br\pi} - \sigma^*$	-0.33
10.31	A''	0.044	$\sigma - \sigma^*$	0.33	8.85	A''	0.01	$n_{Br} - Ryd$	-0.41	8.85	A''	0.01	$n_{\pi} - Ryd$	0.41
			$n_{Br} - 5p$	0.69				$n_{Br} Ryd$	-0.51				$n_{Br\pi} - Ryd$	0.39
			$n_{Br\pi} - Ryd$	0.60				$n_{Br} - Ryd$	-0.51				$n_{\pi} - Ryd$	0.41
			$n_{Br\pi} - \sigma^*$	-0.24				$n_{Br\pi} - Ryd$	-0.51				$n_{Br\pi} - Ryd$	-0.51

دانلود مقاله



<http://daneshyari.com/article/26049>



- ✓ امکان دانلود نسخه تمام متن مقالات انگلیسی
- ✓ امکان دانلود نسخه ترجمه شده مقالات
- ✓ پذیرش سفارش ترجمه تخصصی
- ✓ امکان جستجو در آرشیو جامعی از صدها موضوع و هزاران مقاله
- ✓ امکان پرداخت اینترنتی با کلیه کارت های عضو شتاب
- ✓ دانلود فوری مقاله پس از پرداخت آنلاین
- ✓ پشتیبانی کامل خرید با بهره مندی از سیستم هوشمند رهگیری سفارشات